

This Week in The Journal

● Cellular/Molecular

PIP₂ Regulation of M-Type Potassium Channels

Yang Li, Nikita Gamper, Donald W. Hilgemann, and Mark S. Shapiro

(see pages 9825–9835)

Voltage-gated Kv7 (KCNQ) potassium channels that underlie the M current appear to be modulated by the membrane-bound molecule phosphatidylinositol (4,5)-bisphosphate (PIP₂). This week, Li et al. looked for direct gating of Kv7 channels by PIP₂. The authors measured whole-cell and single-channel currents of Kv7.2, Kv7.3, and Kv7.4 homomultimers and Kv7.2/7.3 heteromultimers. In cell-attached membrane patches, the maximal open probability (P_o) of heteromultimeric channels declined significantly with patch excision. Bath application of the soluble diC8-PIP₂ to the cytoplasmic face of the patch increased P_o . The variable P_o of homomultimeric channels correlated with their response to diC8-PIP₂, suggesting different apparent affinities for PIP₂. Coexpression of phosphatidylinositol 4(5)-kinase, which raises tonic PIP₂ levels, increased the P_o of Kv7 channels, whereas PIP₂-degrading agents decreased whole-cell currents. These results provide additional support for the depletion of PIP₂ by phospholipase C as the mechanism of muscarinic suppression of the M current.

▲ Development/Plasticity/Repair

Integrin $\beta 8$ and CNS Vascular Development

John M. Proctor, Keling Zang, Denan Wang, Rong Wang, and Louis F. Reichardt

(see pages 9940–9948)

The cerebral vasculature plays an important but underappreciated role in the formation of the brain and the blood–brain barrier. One integrin family member, $\alpha v\beta 8$, is required for formation of brain capillaries, and mice lacking $\beta 8$ have severe cerebral hemor-

rhages and premature death. This heteromeric extracellular matrix receptor has several binding partners, including a TGF-1-associated peptide, vitronectin, and laminin. This week, Proctor et al. used a conditional knock-out approach to selectively delete $\beta 8$ from the neuroepithelium, endothelial cells, and migrating neurons. Deletion from the latter two resulted in a normal phenotype, but loss of *itg $\beta 8$* from the neuroepithelium (using *nestin-cre*) caused hemorrhages at birth, suggesting that $\beta 8$ integrin expression on non-neuronal cells was necessary for vascular development. The phenotype in the conditional knock-out was less severe than in *itg $\beta 8$* -null mice. Without neuroepithelial *itg $\beta 8$* , capillaries were morphologically abnormal and astroglial cells were disorganized.

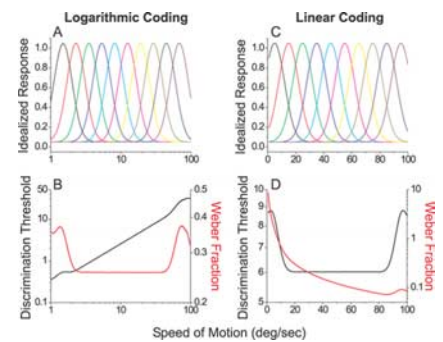
■ Behavioral/Systems/Cognitive

Speed Representation in Macaque MT

Harris Nover, Charles H. Anderson, and Gregory C. DeAngelis

(see pages 10050–10060)

Neurons of the middle temporal (MT) visual area encode perception of not only the direction of motion but also its speed. In humans, the speed discrimination threshold relative to the reference speed (expressed as a ratio called the Weber fraction) is relatively constant across a range of speeds (5–60°/s). The constant Weber fraction allows precision in speed judgments in the setting of changing background speed. This week, Nover et al. tackled the quantitative representation of speed in macaque MT neurons. The authors propose that MT neurons use a logarithmic coding scheme to achieve this task. They recorded from hundreds of MT neurons with various speed preferences. Their analysis indicated that MT neurons displayed Gaussian speed-tuning curves in log speed, and the tuning curves of the population formed a scale-invariant set. The predicted output of the MT population closely matched the human psychophysical data.



Two different schemes for speed discrimination by units in the macaque area MT, logarithmic coding and linear coding. Ten units are shown with constant bandwidth and with sensitivities distributing across a range of speeds. In the bottom panels, for logarithmic coding note the increase in discrimination threshold with the speed of motion, as well as the constant Weber fraction. See the article by Nover et al. for details in favor of logarithmic coding.

◆ Neurobiology of Disease

Microimaging Amyloid Plaques in Mice

Clifford R. Jack Jr, Thomas M. Wengenack, Denise A. Reyes, Michael Garwood, Geoffrey L. Curran, Bret J. Borowski, Joseph Lin, Gregory M. Preboske, Silvina S. Holasek, Gregor Adriany, and Joseph F. Podusko

(see pages 10041–10049)

Preclinical diagnosis and clinical trials in Alzheimer's disease are limited by the lack of a noninvasive diagnostic test. This week, Jack et al. continued efforts to image amyloid plaques using magnetic resonance imaging (MRI). Plaques can be identified histologically by 10 weeks of age in doubly transgenic mice expressing mutant amyloid precursor protein and presenilin 1. The authors compared *in vivo* and *ex vivo* MRI measurements with tissue stained for iron and thioflavin-S (Thio-S), a marker of amyloid plaques. Iron in Thio-S-positive plaques presumably makes plaques visible in MRI. *In vivo*, MRI could not reliably resolve plaques until the mice were 9 months of age, by which time 6% of the plaques had reached the detection threshold of 35 μm in diameter. *Ex vivo* MRI was more sensitive, detecting 20 μm plaques by 3 months of age. Plaque detection by MRI still lacks the sensitivity to be useful in humans, but this study identifies some of the unresolved issues.